THE JOURNAL OF BIOLOGICAL CHEMISTRY VOL. 285, NO. 15, pp. 11290–11296, April 9, 2010

Studies of the Maltose Transport System Reveal a Mechanism for Coupling ATP Hydrolysis to Substrate Translocation without Direct Recognition of Substrate*[S]

Received for publication, November 25, 2009, and in revised form, January 19, 2010 Published, JBC Papers in Press, February 10, 2010, DOI 10.1074/jbc.M109.089078

Alister D. Gould and Brian H. Shilton[1]

From the Department of Biochemistry, University of Western Ontario, London, Ontario N6B 2G3, Canada

The ATPase activity of the maltose transporter ($MalFGK_2$) is dependent on interactions with the maltose-binding protein (MBP). To determine whether direct interactions between the translocated sugar and $MalFGK_2$ are important for the regulation of ATP hydrolysis, we used an MBP mutant (sMBP) that is able to bind either maltose or sucrose. We observed that maltose- and sucrose-bound sMBP stimulate equal levels of $MalFGK_2$ ATPase activity. Therefore, the ATPase activity of $MalFGK_2$ is coupled to translocation of maltose solely by interactions between $MalFGK_2$ and MBP. For both maltose and sucrose, the ability of sMBP to stimulate the $MalFGK_2$ ATPase was greatly reduced compared with wild-type MBP, indicating that the mutations in sMBP have interfered with important interactions between MBP and $MalFGK_2$. High resolution crystal structure analysis of sMBP shows that in the closed conformation with bound sucrose, three of four mutations are buried, and the fourth causes only a minor change in the accessible surface. In contrast, in the open form of sMBP, all of the mutations are accessible, and the main chain of Tyr^{62}–Gly^{69} is destabilized and occupies an alternative conformation due to the W62Y mutation. On this basis, the compromised ability of sMBP to stimulate ATP hydrolysis by $MalFGK_2$ is most likely due to a disruption of interactions between $MalFGK_2$ and the open, rather than the closed, conformation of sMBP. Modeling the open sMBP structure bound to $MalFGK_2$ in the transition state for ATP hydrolysis points to an important site of interaction and suggests a mechanism for coupling ATP hydrolysis to substrate translocation that is independent of the exact structure of the substrate.

ATP-binding cassette (ABC)[2] transporters move various substrates across membranes, with substrate movement coupled to the hydrolysis of ATP. Although the ATPase activity of ABC exporters like P-glycoprotein is generally stimulated by substrate binding, the ATPase activity of ABC importers is activated by a peripheral substrate-binding protein and not the free substrate (for recent reviews see Refs. 1–3). However, the mechanism of ATPase regulation is still not fully understood. Here, we use one of the most well studied ABC importers, the *Escherichia coli* maltose transporter ($MalFGK_2$), to investigate the roles of maltose-binding protein (MBP) and maltose itself in regulation of ATPase activity.

In its resting state $MalFGK_2$ contains a substrate-binding site that is exposed to the cytoplasm (4). In the periplasm, MBP binds maltose, which stabilizes a change from an "open" to a "closed" conformation, enabling it to stimulate the $MalFGK_2$ ATPase (5, 6). Interactions with closed, maltose-bound MBP lead to exposure of the $MalFGK_2$ maltose-binding site to the periplasmic side where maltose can move from MBP into an occluded translocation pathway (7, 8). After ATP hydrolysis, the transporter returns its binding site to the cytoplasmic face to allow the substrate to enter the cytoplasm. This is known as the alternating access model of maltose transport (4) and may be a common mechanism among ABC transporters (2, 9, 10).

The structure of a transition state complex between MBP and $MalFGK_2$, as well as biochemical data (7, 8), indicates that maltose enters the substrate-binding site of $MalFGK_2$ prior to ATP hydrolysis, but it is unclear how maltose-bound MBP activates the $MalFGK_2$ ATPase (11) and how ATP hydrolysis is coupled to the movement of maltose across the membrane. Of particular interest are the roles that maltose itself might play in regulating the ATPase activity of $MalFGK_2$.

There are two ways maltose could regulate ATP hydrolysis. The first is by stabilizing the closed conformation of MBP, and the second is through direct interactions with $MalFGK_2$. Although it is clear from previous studies that substrate-induced domain closure in MBP is critical for robust stimulation of the $MalFGK_2$ ATPase and substrate transport (6), it is not known whether direct interaction between maltose and $MalFGK_2$ is also required for ATPase activity.

To address this question, we have used an MBP mutant that is able to bind an alternative substrate, sucrose, with high affinity (12). The sucrose-binding MBP (sMBP) enables us to present the maltose transporter with either maltose or sucrose in equivalent contexts and distinguish whether the substitution influences the ATPase activity of $MalFGK_2$. Sucrose is a good alternative substrate for this purpose because experiments by Shuman and co-workers (13, 14) have shown that it has a very poor ability to compete for the maltose-binding site in $MalFGK_2$, indicating that the change in sugar structure is sufficient to disrupt specific binding interactions with $MalFGK_2$.

* This work was supported by Discovery Grant 217494-2008 from the Natural Sciences and Engineering Research Council of Canada.

[S] The on-line version of this article (available at http://www.jbc.org) contains supplemental Figs. S1 and S2.

The atomic coordinates and structure factors (codes 3KJT and 3HPI) have been deposited in the Protein Data Bank, Research Collaboratory for Structural Bioinformatics, Rutgers University, New Brunswick, NJ (http://www.rcsb.org/).

[1] To whom correspondence should be addressed: Dept. of Biochemistry, University of Western Ontario, 1151 Richmond St., London, Ontario N6B 2G3, Canada. Tel.: 519-661-4124; Fax: 519-661-3175; E-mail: bshilton@uwo.ca.

[2] The abbreviations used are: ABC, ATP-binding cassette; MBP, maltose-binding protein; sMBP, sucrose-binding MBP; PDB, Protein Data Bank.

Using sMBP, we have determined that ATP hydrolysis by $MalFGK_2$ is not dependent on the exact nature of the substrate, and therefore the coupling of ATPase activity to substrate translocation is due solely to interactions between MBP and $MalFGK_2$. Based on these findings and detailed structural analysis of sMBP, we propose that a productive interaction between MalG and the vacated maltose-binding site in MBP is required for ATP hydrolysis. In this manner, substrate translocation from MBP to $MalFGK_2$ is coupled to ATP hydrolysis without requiring a direct interaction between maltose and $MalFGK_2$.

MATERIALS AND METHODS

Cloning of MBP Mutants—Plasmid pDIM-C8MalE, containing sMBP, was kindly provided by Ostermeier and co-workers (12). A 923-bp Kpn21/BclI fragment of this vector, containing the W62Y and E111Y substitutions, was ligated into pLH1, which contains the MBP signal sequence for export to the periplasm. The D14L and K15F mutations were substituted by mutagenic PCR using the following primers: 5′-CTGGATTAACGGCCTTTTCGGCTATAACGGTCTCGC-3′ and 5′-GCGAGACCGTTATAGCCAAAAAGGCCGTTAATCCAG-3′.

To produce intracellularly expressed sMBP and wtMBP with a hexahistidine affinity tag, restriction cut sites for EheI and HindIII were added to excise the two genes (without localization tag) using the following primers: 5′-CGCCTCGGCTGGCGCCAAAATCGAAG-3′ and 5′-CGCCGCATCCGGCATTTAAGCTTATTACTTGGTGATACGAG-3′. Digested PCR products were then ligated into the multicloning site of pPROEX-HTa (Invitrogen) to introduce an N-terminal hexahistidine tag attached by a tobacco etch virus protease cleavable linker. Cleavage of this linker left an N-terminal glycine-alanine insertion that was common to both the sMBP and wtMBP used in this study.

Expression and Purification—Hexahistidine-tagged sMBP and wtMBP were expressed and purified from HS3309 ($MalE^{-/-}$) *E. coli* by Ni^{2+}-affinity chromatography, removal of the affinity tag by tobacco etch virus protease cleavage, and ion exchange chromatography, as reported previously (15). Both proteins were denatured in 6 M guanidine and dialyzed exhaustively to remove trace sugars before being refolded by dropwise dilution and stored at −80 °C in 50 mM Tris-HCl, pH 8 (15).

Preparation of wt-$MalFGK_2$-containing Proteoliposomes—$MalFGK_2$ was overexpressed from plasmids $pNT1SK^+$ and pMR111 in *E. coli* HS3399 cells, which contain deletions for all transporter components. Membrane fractions were prepared and solubilized as reported previously (15).

Liposomes were prepared from Avanti™ crude *E. coli* phospholipids, and after homogenization by sonication, the liposomes were combined with $MalFGK_2$-containing membranes by detergent dilution (15). The proteoliposomes were frozen at −80 °C under N_2 until used.

ATPase Assays—ATPase measurements were made in a solution of 50 mM Tris-HCl, pH 8.0, 100 mM KCl, and 10 mM $MgCl_2$, with proteoliposomes added to a final concentration of 0.1 mg/ml protein. Purified sMBP or wtMBP was added at various concentrations and in the presence or absence of 5 mM maltose or sucrose. ATP hydrolysis at 37 °C was measured *in vitro* by assaying the appearance of inorganic phosphate, using ammonium molybdate, as described previously (15).

Crystallization and X-ray Diffraction—Crystals of sucrose-bound sMBP were grown in 21% PEG 3350K, 100 mM sodium acetate, pH 6.5, 60 mM $MgCl_2$, and 10 mM $ZnCl_2$ with 100 mM sucrose. Crystals of unliganded sMBP were grown from PEG 5k-MME, sodium acetate, pH 6.5, 60 mM $MgCl_2$, and 10 mM $ZnCl_2$. Crystals of sucrose-bound and unliganded sMBP diffracted to 2 and 1.5 Å, respectively, at the Canadian Light Source beamline CMCF1 (08ID-1).

Phases were determined by molecular replacement with the wild-type proteins (PDB codes 1ANF and 1OMP). Rigid body refinement of the two isolated domains was carried out first to capture any domain movements relative to the wild-type structures. Structures were refined using CNS (Table 1) (22) with manual adjustment in COOT (23). The structures have been deposited in the PDB with codes 3KJT and 3HPI for the open and closed forms, respectively. Molecular figures were made using PyMOL (24).

RESULTS

Sucrose-binding MBP—sMBP is a mutant form of MBP developed by Ostermeier and co-workers (12). The sMBP molecule has four point mutations, D14L, K15F, W62Y, and E111Y, all within the substrate binding cleft. Although wild-type MBP (wtMBP) has a dissociation constant (K_D) of 1 μM for maltose and no ability to bind sucrose (6), sMBP has a K_D for maltose of 24 μM and for sucrose of 6.6 μM (12). These values were confirmed for our sMBP constructs using fluorescence titrations (data not shown). Furthermore, we measured substrate-induced conformational changes in sMBP, in solution, by small angle x-ray scattering. Sucrose-induced changes in the conformation of sMBP were identical to changes seen in wtMBP (supplemental Fig. S1), with the ligand-bound and unliganded conformations of sMBP clearly matching the ligand-bound and unliganded conformations of wtMBP, respectively (data not shown). We also observed that sMBP could complement the growth of wtMBP-deficient *E. coli* on M9 maltose minimal media (data not shown). Although growth with sMBP was 3–4 times slower compared with that observed with wtMBP, in control experiments with no binding protein, there was no growth. Therefore, sMBP interacts productively with $MalFGK_2$ to promote maltose transport.

sMBP stimulates $MalFGK_2$ with Bound Sucrose or Maltose—$MalFGK_2$ has a binding site that is relatively specific for maltodextrins (13), and binding of the substrate to this site may be important for stimulation of the $MalFGK_2$ ATPase. To determine the importance of specific interactions between maltose and $MalFGK_2$, we used sMBP to present $MalFGK_2$ with either maltose or sucrose as a transport substrate and measured the resulting stimulation of ATPase activity *in vitro*. Consistent with literature findings, $MalFGK_2$-containing proteoliposomes showed a low level of basal activity (Fig. 1). This activity was unaltered by the addition of 5 mM maltose or sucrose, confirming that free sugar cannot stimulate the transporter in the absence of MBP (data not shown; see Ref. 11). When 20 μM sMBP was added to wild-type $MalFGK_2$, no statistically signif-

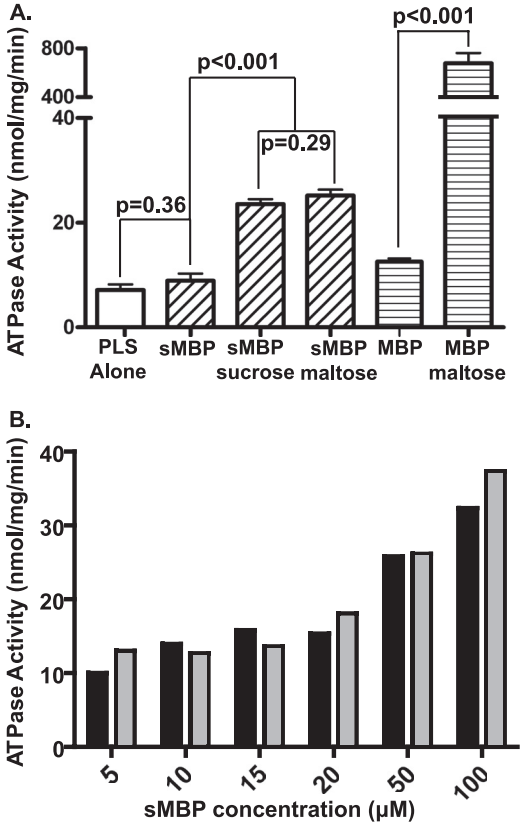

FIGURE 1. **Effect of ligand on stimulation of the MalFGK$_2$ ATPase.** MalFGK$_2$ was reconstituted into a proteoliposome system (*PLS*), and the effects of MBP and ligands on the MalFGK$_2$ ATPase were measured. *A,* proteoliposome systems have a basal ATPase (*clear bar*) that is not significantly increased by unliganded sMBP. When bound to either sucrose or maltose, sMBP produces a 3-fold stimulation over the basal rate (*bars* with *diagonal lines*). The much larger ATPase stimulation by 20 μM wtMBP (*bars* with *horizontal lines*) shows that the mutations in sMBP have impaired its ability to stimulate the MalFGK$_2$ ATPase compared with wtMBP. *B,* abilities of sucrose-sMBP (*black*) and maltose-sMBP (*gray*) to stimulate MalFGK$_2$ above its basal ATPase were compared over a range of sMBP concentrations; the sugars were present at a concentration of 5 mM.

TABLE 1
Crystallographic statistics

	sMBP-sucrose	Unliganded sMBP
PDB codes	3HPI	3KJT
Resolution limit	2.0 Å	1.5 Å
Space group	$P2_12_12_1$	$P2_1$
Unit cell parameters		
a, *b*, *c*	60.042, 85.229, 132.864 Å	43.888, 65.544, 57.5 Å
α, β, γ	90, 90, 90°	90, 101.141, 90°
Molecules per asymmetric unit	2	1
Solvent content	0.41	0.4
Unique reflections	44813	48552
Mean $I/(\sigma I)$[a]	16.1 (2.38)	17.8 (2.03)
R_{merge}[a]	0.092 (0.468)	0.048 (0.329)
Completeness[a]	96.2% (86.4%)	88.1% (58.5%)
Redundancy[a]	5.8 (4.4)	3.3 (2.2)
No. of reflections		
Total	40,799	43,724
R_{free}	2032	2345
Refinement		
Resolution range	34.8–2.0 Å	24.8–1.5 Å
R_{work}	0.228	0.215
R_{free}	0.284	0.243
r.m.s.d.[b] bond length	0.00621 Å	0.00497 Å
r.m.s.d. bond angle	1.22°	1.17°
***B* factors**		
Protein	34.2 Å^2	16.7 Å^2
Ligand	29.1 Å^2	N/A Å^2
Solvent	33.1 Å^2	25.2 Å^2
Ramachandran analysis		
Most favored	92%	91%
Allowed	8%	9%
Generously allowed	0	0
Disallowed	0	0

[a] Values in parentheses refer to the highest resolution shell.
[b] r.m.s.d. is root mean square deviation.

icant increase in activity was observed. However, in the presence of either 5 mM maltose or sucrose, sMBP stimulated a 3-fold increase in ATP hydrolysis over background (Fig. 1*A*, *bars* with *diagonal lines*). We have therefore observed that, with respect to ATPase activation, MalFGK$_2$ cannot distinguish sucrose from maltose. To demonstrate that the equivalence of maltose- and sucrose-bound sMBP was not limited to 20 μM sMBP concentration, a range of concentrations, from 1 to 100 μM, was tested (Fig. 1*B*). Across this concentration range, maltose- and sucrose-bound sMBP stimulate the MalFGK$_2$ ATPase to similar levels; the overall trend (in both cases a proportional increase in MalFGK$_2$ ATPase activity as sMBP concentration is raised) suggests that the mechanism for stimulation is the same, irrespective of the sugar with which MalFGK$_2$ comes into contact.

Although maltose- and sucrose-bound sMBP both stimulate the MalFGK$_2$ ATPase to the same extent, the absolute levels of ATPase activity produced by sMBP were much lower than those produced by wtMBP. For example, in the presence of maltose, the level of ATPase stimulation by 20 μM wtMBP was 40-fold higher than the stimulation produced by the same concentration of either maltose- or sucrose-bound sMBP. In addition, unliganded sMBP did not produce a significant increase in MalFGK$_2$ ATPase, in contrast to unliganded wtMBP that consistently produces a 2-fold stimulation (Fig. 1*A*) (11, 15). Therefore, although the substitution of sucrose for maltose did not influence stimulation of the MalFGK$_2$ ATPase, when compared with wtMBP the mutations in sMBP have drastically compromised its overall ability to stimulate the MalFGK$_2$ ATPase.

Structural Analysis of Open and Closed sMBP—To determine how the mutations in sMBP disrupt its ability to stimulate MalFGK$_2$, we solved the crystal structures of sMBP in both the sucrose-bound and substrate-free forms to resolutions of 2.0 and 1.5 Å, respectively (Table 1). In both forms sMBP adopts a wild-type fold, with main chain atoms differing from wtMBP by a root mean square deviation for Cα positions of 0.48 Å in the closed form and 0.55 Å in the open form.

Well defined electron density for sucrose was seen in the binding site of the sMBP sucrose structure; the electron density clearly defines each hydroxyl group of sucrose and does not fit maltose (Fig. 2*A*). Like maltose-bound wtMBP, sMBP binds sucrose through hydrogen bonds with each of the two sugar rings. The first nonreducing glucose unit is common to both maltose and sucrose and occupies an identical binding pocket in wtMBP and sMBP (Fig. 2*B*). The second sugar ring differs between maltose and sucrose, being an α-1,4-linked reducing glucose in maltose and an α-1,2-linked fructose in sucrose; as a result, sucrose adopts a 90° bend compared with maltose. This bend allows the C3 hydroxyl to hydrogen bond with residue W62Y, which was likely selected for this purpose (Fig. 2*B*). The

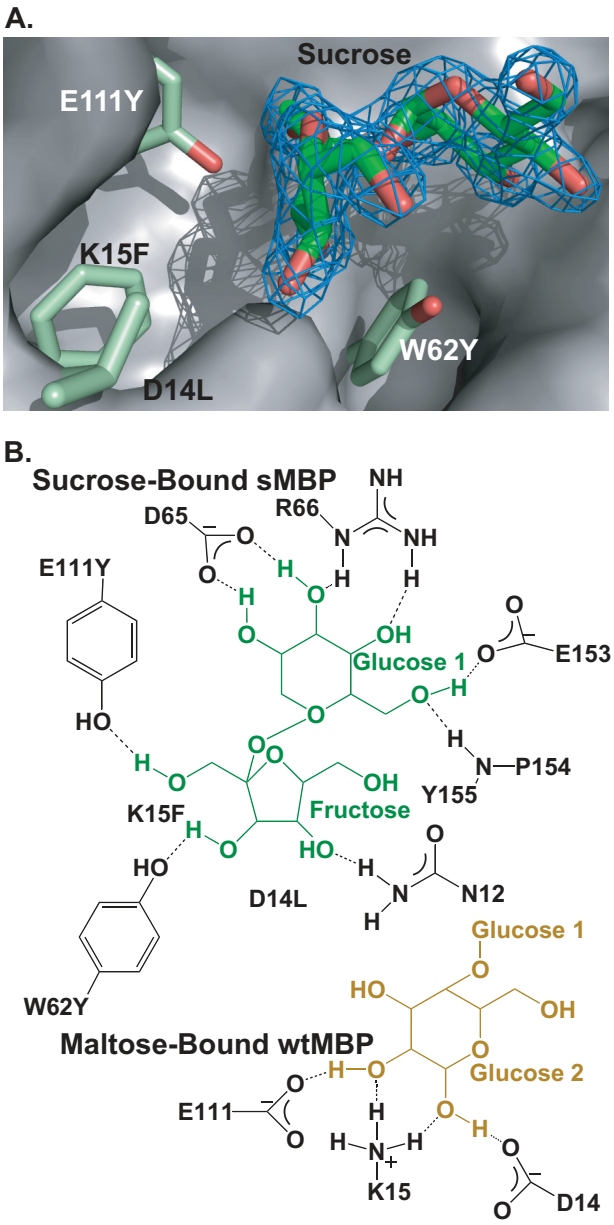

bend also creates a cavity in the binding site and separates the sugar from residues 14 and 15 (Fig. 2*C*). The D14L, K15F, and E111Y mutations modify this hydrophobic cavity by removing what would otherwise be unmatched buried charges or polar groups.

We also solved the crystal structure of the open conformation of sMBP to 1.5 Å resolution and were surprised to find a significant change in the structure of the ligand-binding site. The W62Y mutation is able to adopt an alternative conformation that displaces the main chain segment from residues Tyr^{62} to Gly^{69} (Fig. 3). This difference was evident from clear electron density for the Tyr^{62} side chain in two different places, one of which necessarily displaces Phe^{67} and is therefore incompatible with the wild-type main chain conformation (Fig. 3*C*). The only way this change can be accommodated is for residues 62–69 to partially extend into the substrate binding cleft. The occupancies of the two conformations of residues 66–69 were set such that the temperature factors for the wild-type conformation are similar to the main chain average, as is the case with open, wild-type MBP (5). On this basis, the occupancy of the wild-type conformation is estimated at 0.4 and that of the alternative conformation is 0.6.

Both the open and closed conformations of MBP are involved in maltose transport (8, 14–16). To understand why sMBP has such a compromised ability to stimulate the $MalFGK_2$ ATPase, we compared its surface in both the open and closed conformations to that of wtMBP. The changes in sMBP necessary to support sucrose binding require only side chain substitutions, most of which are buried in the sugar-binding site and are not surface accessible in the closed form of the protein. As a result, the surface morphology of closed sMBP is virtually unaltered from closed wtMBP (Fig. 4*A*), with only a slight perturbation caused by the exposure of a methyl group on D14L (supplemental Fig. S2).

In contrast to the closed state, the open conformation of sMBP fully exposes all four binding site mutations to the solvent (Fig. 4*B*) as well as the alternative and partially disordered conformations for residues 62–69, caused by the W62Y mutation (Fig. 3). To summarize, our structural analysis found that in the sucrose-bound closed form, sMBP closely mimics the surface morphology of wtMBP, but open unliganded sMBP displays a drastically altered sugar-binding site.

FIGURE 2. **Sucrose binding by sMBP.** The structure of sucrose-bound sMBP was solved and refined to 2 Å resolution (Table 1); coordinates for wtMBP and maltose were from PDB code 1ANF (25). *A,* bound sucrose (*dark green*) and the mutated residues (*pale green*) are shown, along with $2F_o - F_c$ electron density for the sucrose (*blue mesh*) contoured at 2σ. The electron density map was calculated using phases from the partially refined structure, prior to the addition of sucrose to the binding site. *B,* hydrogen bonding interactions between sucrose and sMBP (*top*) are compared with those between maltose and wtMBP (*bottom*). Hydrogen bonding interactions to the first glucose ring are the same for both proteins. *C,* comparison of the ligand-binding sites of sMBP and wtMBP. The molecular surface that sMBP and wtMBP have in common is shown in *gray*; carbon atoms from maltose and wtMBP are shown in *orange* and *yellow*, respectively, and those from sucrose and sMBP are shown in *dark green* and *pale green*. The conformation of sucrose creates a cavity that would normally be filled with atoms from the second glucose unit of maltose, to which three charged residues (Asp^{14}, Lys^{15}, and Glu^{111}) would be hydrogen-bonded, as illustrated in *B*. The mutations in sMBP (*pale green*) convert these three charged residues to neutral residues.

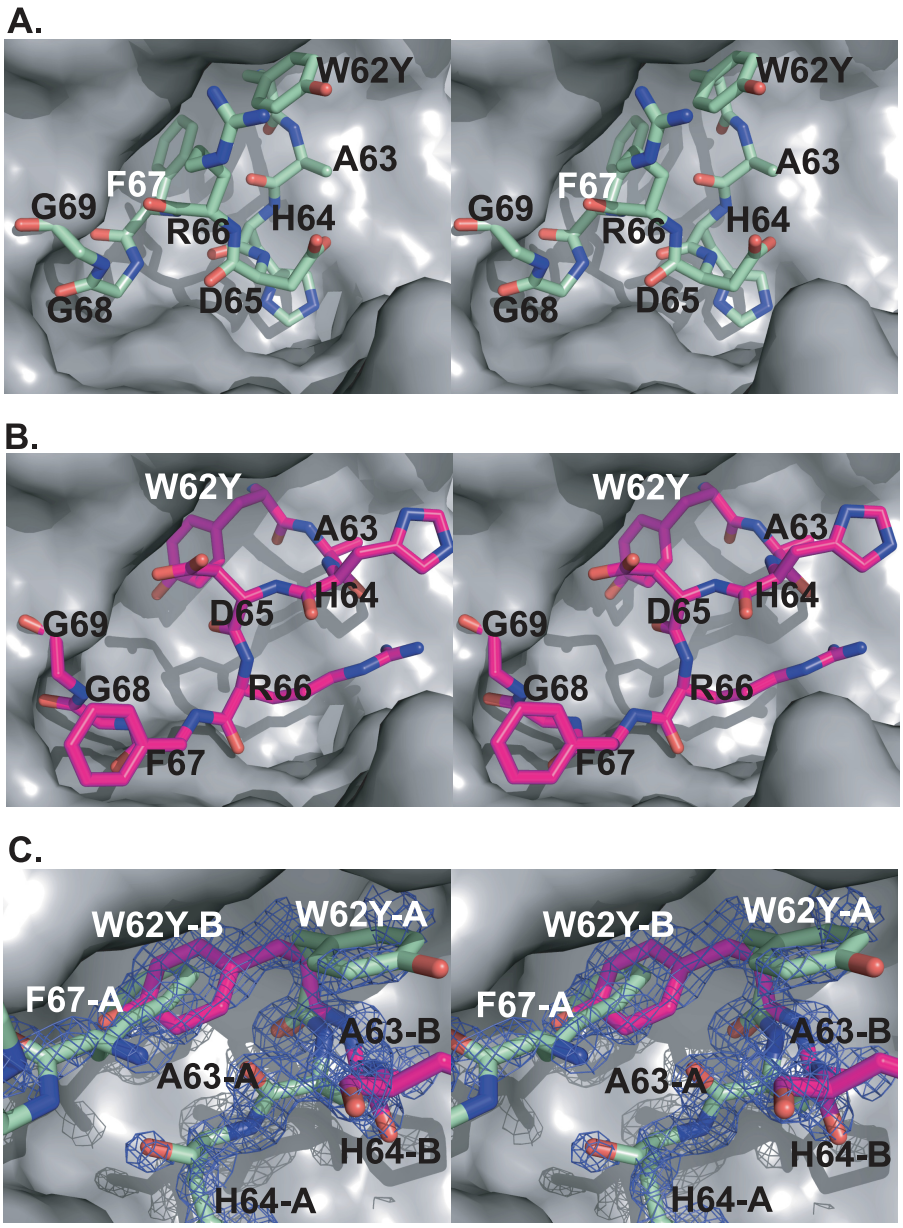

FIGURE 3. **Main chain disorder in the open unliganded sMBP structure.** Residues 62–69 adopt two different conformations in the open, unliganded structure of sMBP, which was refined to 1.5 Å resolution (Table 1). The molecular surface of sMBP (excluding residues 62–69) is shown with residues 62–69 included as stick models in either the conformation resembling that observed in wtMBP (*A*) or the alternative conformation observed in sMBP (*B*). *C*, superposition of the two conformations observed in sMBP, along with $2F_o - F_c$ electron density calculated from phases obtained through a simulated annealing procedure with residues 62–69 omitted from the structure. Note the electron density for Tyr^{62} in two different positions. The A position for Tyr^{62} corresponds to the position of Trp^{62} in wtMBP; occupancy of the B position requires an alternative conformation for the main chain residues.

Altered Interactions between Open sMBP and MalFGK$_2$—To investigate how the mutations in open sMBP could cause such a drastic defect in its ability to stimulate the MalFGK$_2$ ATPase, we replaced wtMBP with sMBP in the crystal structure of MBP-MalFGK$_2$ that corresponds to the transition state for ATP hydrolysis (7, 8). The backbone positions of sMBP fit the MBP component of the trapped transition state to a root mean square deviation of 0.84 Å.

The binding of sMBP to the transporter transmembrane (MalFG) domains was not obviously compromised across the exterior surface of the binding protein, including contacts between sMBP and the MalF P2 arm (17, 18). However, mutations D14L, W62Y, and E111Y disrupted interactions of the maltose-binding site with residues 253–258 of MalG, which occupy the maltose-binding site in the transporter transition state (Fig. 5). These residues include an invasive structure known as the MalG P3 "scoop loop," named for its probable role in excluding maltose from the ligand-binding site in MBP (8). A previous study showed that a 31-residue insertion into this loop did not affect assembly of MalFGK$_2$ but abolished transport by the system by disrupting interactions with MBP (19). In the case of the interaction with sMBP, D14L clashes with Asn^{254} of MalG, whereas W62Y and E111Y remove stabilizing van der Waals and hydrogen bond interactions. In addition, the alternative conformation adopted by residues 62–69 will interfere with MalG interactions. Altogether, the mutations in the open conformation of sMBP would be expected to disrupt interactions with the MalG P3 loop in the transition state for ATP hydrolysis.

In summary, the mutations in sMBP have a drastic effect on its ability to stimulate MalFGK$_2$ ATPase activity. Structural analysis indicates that this effect is due to a disruption of interactions between residues 253 and 258 of MalG and the empty sugar-binding site of MBP as it occurs in the transition state for ATP hydrolysis. The magnitude of this effect shows that these interactions are critical for stimulation of the MalFGK$_2$ ATPase.

DISCUSSION

We observed that a sucrose-binding mutant of MBP was able to stimulate the ATPase activity of MalFGK$_2$ with either maltose or sucrose present as substrate. Although the level of stimulation by sMBP was only 2–3% of that produced by wtMBP, we believe the system is operating along the same reaction pathway as the fully wild-type system. The ATPase measurements were carried out in a well characterized proteoliposome system in which the ATPase activity of MalFGK$_2$ is tightly coupled to interactions with MBP. Because MalFGK$_2$ is wild type, and sMBP adopts the same open and closed structures as wtMBP, the conformational changes in the system as a whole will be similar for sMBP and wtMBP. In

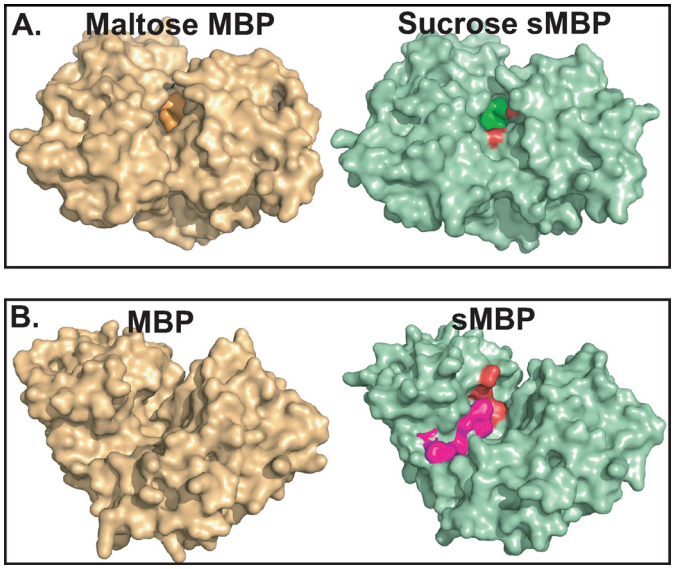

FIGURE 4. **Effect of mutations on the surface properties of open and closed sMBP.** The molecular surfaces of wtMBP (*tan*) and sMBP (*pale green*) are compared for both the closed (*A*) and open conformations (*B*). In the closed conformation, the surfaces of bound maltose and sucrose are colored *orange* and *dark green*, respectively. The D14L and W62Y mutations are visible (*red patches*) but have very little effect on the accessible surface of sMBP compared with wtMBP. *B,* in the open conformation, all of the mutations are visible (*red patches*). In addition, the main chain residues 62–69 are partially disordered; the alternative conformation for these residues is shown in *magenta*. Coordinates for open and closed wtMBP correspond to 1OMP (5) and 1ANF (25), respectively.

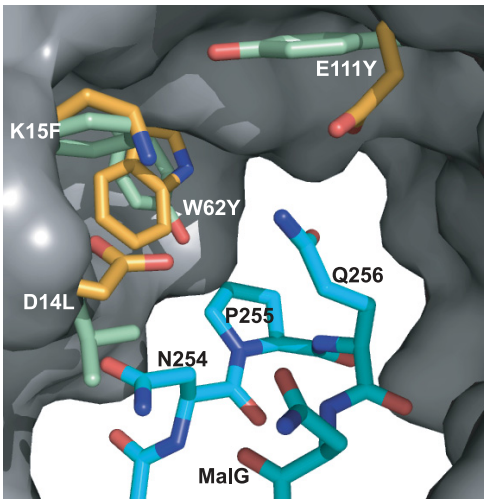

FIGURE 5. **Interactions between the MalFGK$_2$ P3 loop and the sMBP ligand-binding site.** The open conformation of sMBP was superimposed onto wtMBP in the transition state structure of the MBP-MalFGK$_2$ complex (PDB code 2R6G (8)). Residues 254–257 of MalG (*cyan*) extend into the sugar-binding site, making contacts with wtMBP residues 14, 62, and 111 (*yellow*). The contacts made between MalG and the ligand-binding site would be affected by the mutations in sMBP. In addition, interaction with the MalG P3 loop would be disrupted due to disorder in sMBP residues 62–69, as outlined in Fig. 3.

addition, sMBP is able to mediate growth on minimal maltose media, showing that the sMBP-stimulated ATPase activity is associated with maltose transport *in vivo*.

The activation by sMBP was indistinguishable between maltose and the nonphysiological substrate sucrose. The available evidence suggests that sucrose is unable to interact with the maltose-binding site in MalFGK$_2$. For example, in transport assays using MBP-independent MalFGK$_2$ mutants, sucrose was incapable of competitively inhibiting the transport of maltose (13) indicating that the substrate-binding site of MalFGK$_2$ has little, if any, affinity for sucrose. This can be explained using the MalFGK$_2$ structure in complex with maltose (8); modeling sucrose into the same position as maltose results in clashes with MalF residues 383, 433, and 436, including steric clashes with backbone atoms. Because sucrose is unable to occupy the maltose-binding site of MalFGK$_2$, the observation that maltose- and sucrose-bound sMBP have equal abilities to stimulate MalFGK$_2$ demonstrates that specific binding of the carbohydrate by MalFGK$_2$ is not important for activation of its ATPase. Therefore, it is the substrate-induced conformational change in MBP, but not the identity of the substrate itself, that is critical for stimulation of the MalFGK$_2$ ATPase.

In principle, ATP-dependent transporters should couple ATP hydrolysis to the actual movement of substrate. Our results with sMBP show that direct interactions with the substrate are not required for stimulation of the MalFGK$_2$ ATPase, and therefore coupling of ATP hydrolysis to substrate translocation must depend solely on interactions between MBP and MalFGK$_2$. In this regard, the very strong defect in the ability of sMBP to stimulate the MalFGK$_2$ ATPase indicates that a critical interaction between MBP and MalFGK$_2$ has been disrupted by the mutations.

Both the open and closed conformations of MBP interact with MalFGK$_2$ during the catalytic cycle (3, 7, 8, 15). The surface of closed sMBP is almost identical to that of wtMBP, suggesting that this conformation is not responsible for the reduced ability of sMBP to stimulate the MalFGK$_2$ ATPase. In fact, Leu^{14} (Asp^{14} in wtMBP) is the only mutant residue that causes a change in the exposed surface of closed sMBP and could therefore alter interactions with MalFGK$_2$. Although functional genetic screens have demonstrated that the region around residue 14 is important for the interaction of MBP and MalFGK$_2$ (20, 21), the only change found at residue 14 in the genetic screens was a mutation to tyrosine, a much larger residue that cannot be buried in the ligand-bound conformation of MBP and would therefore produce a large change in the surface of the closed conformation. In contrast, the D14L mutation is mostly buried and almost isosteric (supplemental Fig. S2), resulting in only a very small change in the surface, namely a 2-Å extension of an existing hydrophobic patch (supplemental Fig. S2). Therefore, the small effect of the D14L mutation on the surface of closed sMBP does not provide a convincing explanation for the profound effect of the mutations on the ability of sMBP to stimulate MalFGK$_2$.

The surface of open sMBP, on the other hand, is drastically altered by the exposure of mutant residues in the sugar-binding site and the creation of an area of conformational instability due to the W62Y mutation. On this basis, the profound defect in sMBP is most likely due to a disruption of interactions between the open, rather than the closed, conformation of MBP. This conclusion is consistent with an important role for open MBP in stabilization of the transition state for ATP hydrolysis (8, 15).

In fact, the reduced activation of MalFGK$_2$ ATPase by sMBP coincides with a disruption of interactions between sMBP ligand-binding site residues and the invasive MalG P3 loop of

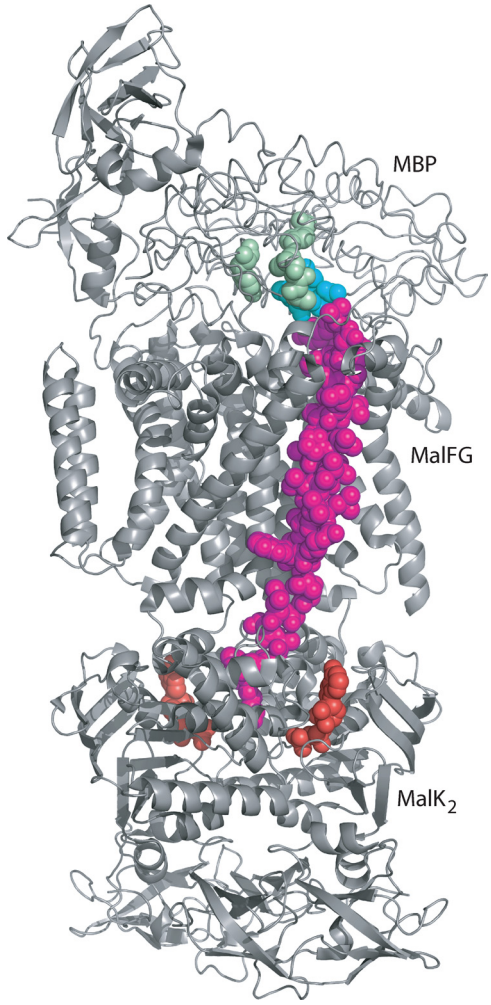

FIGURE 6. **Structural basis for communication between the MalG P3 loop and ATP binding cassettes.** The MBP-MalFGK$_2$ transition state complex (PDB code 2R6G (8)) is shown. As detailed in Fig. 5, MalG residues 254–257 (*cyan*) make contacts with the mutated residues (*green*) in the sugar-binding site of MBP. These contacts are only possible when maltose is absent, hence the term "scoop loop" was used to assign a function to this region of MalG (8). The loop is connected with the MalK$_2$ ATP-binding sites (*red*) via the MalG C terminus (*magenta*).

MalFGK$_2$ (8). These interactions are only possible once MBP adopts the open conformation and maltose has vacated the MBP sugar-binding site to enter MalFGK$_2$. The interactions between the MalG P3 loop and the ligand-binding site of MBP appear to play a critical role in transport coupling by allowing hydrolysis of ATP only once the ligand has translocated from the binding site in MBP to the MalFGK$_2$-binding site.

A role for the MalG P3 loop in energetic coupling is consistent with its position in MalFGK$_2$ (Fig. 6). The P3 loop is connected to MalG helices 15 and 16, which extend from the scoop loop to the MalG C terminus, located in a hydrogen bond network equidistant between the two ATP-binding sites of MalK$_2$. Our data indicate that in addition to extracting maltose from the MBP sugar binding cleft (8), interactions between the MalG P3 loop and MBP also play a direct role in promoting ATP hydrolysis. These interactions do not depend on the specific chemical identity of the substrate, and therefore a similar mechanism might be operative in multidrug exporters and other ABC transporters that couple ATP hydrolysis to the transport of diverse substrates.

Acknowledgments—We thank Lee-Ann Briere and Dr. Stanley Nithianantham for help with crystallization and data collection, and Dr. Marc Ostermeier for providing the expression construct for sMBP. Crystallographic data were collected at the Canadian Light Source, which is supported by Natural Sciences and Engineering Research Council of Canada, National Research Council, Canadian Institutes of Health Research, and the University of Saskatchewan. Use of the Advanced Photon Source is supported by the United States Department of Energy, Basic Energy Sciences, Office of Science, under Contract W-31-109-ENG-38, and BioCAT is supported by National Institutes of Health Research Grant RR-08630.

REFERENCES

1. Davidson, A. L., Dassa, E., Orelle, C., and Chen, J. (2008) *Microbiol. Mol. Biol. Rev.* **72,** 317–364
2. Jones, P. M., O'Mara, M. L., and George, A. M. (2009) *Trends Biochem. Sci.* **34,** 520–531
3. Shilton, B. H. (2008) *Biochim. Biophys. Acta* **1778,** 1772–1780
4. Khare, D., Oldham, M. L., Orelle, C., Davidson, A. L., and Chen, J. (2009) *Mol. Cell* **33,** 528–536
5. Sharff, A. J., Rodseth, L. E., Spurlino, J. C., and Quiocho, F. A. (1992) *Biochemistry* **31,** 10657–10663
6. Hall, J. A., Thorgeirsson, T. E., Liu, J., Shin, Y. K., and Nikaido, H. (1997) *J. Biol. Chem.* **272,** 17610–17614
7. Austermuhle, M. I., Hall, J. A., Klug, C. S., and Davidson, A. L. (2004) *J. Biol. Chem.* **279,** 28243–28250
8. Oldham, M. L., Khare, D., Quiocho, F. A., Davidson, A. L., and Chen, J. (2007) *Nature* **450,** 515–521
9. Dawson, R. J., Hollenstein, K., and Locher, K. P. (2007) *Mol. Microbiol.* **65,** 250–257
10. Hollenstein, K., Frei, D. C., and Locher, K. P. (2007) *Nature* **446,** 213–216
11. Davidson, A. L., Shuman, H. A., and Nikaido, H. (1992) *Proc. Natl. Acad. Sci. U.S.A.* **89,** 2360–2364
12. Guntas, G., Mansell, T. J., Kim, J. R., and Ostermeier, M. (2005) *Proc. Natl. Acad. Sci. U.S.A.* **102,** 11224–11229
13. Shuman, H. A. (1982) *J. Biol. Chem.* **257,** 5455–5461
14. Merino, G., and Shuman, H. A. (1997) *J. Bacteriol.* **179,** 7687–7694
15. Gould, A. D., Telmer, P. G., and Shilton, B. H. (2009) *Biochemistry* **48,** 8051–8061
16. Bohl, E., Shuman, H. A., and Boos, W. (1995) *J. Theor. Biol.* **172,** 83–94
17. Daus, M. L., Grote, M., and Schneider, E. (2009) *J. Bacteriol.* **191,** 754–761
18. Grote, M., Polyhach, Y., Jeschke, G., Steinhoff, H. J., Schneider, E., and Bordignon, E. (2009) *J. Biol. Chem.* **284,** 17521–17526
19. Nelson, B. D., and Traxler, B. (1998) *J. Bacteriol.* **180,** 2507–2514
20. Hor, L. I, and Shuman, H. A. (1993) *J. Mol. Biol.* **233,** 659–670
21. Treptow, N. A., and Shuman, H. A. (1988) *J. Mol. Biol.* **202,** 809–822
22. Brünger, A. T., Adams, P. D., Clore, G. M., DeLano, W. L., Gros, P., Grosse-Kunstleve, R. W., Jiang, J. S., Kuszewski, J., Nilges, M., Pannu, N. S., Read, R. J., Rice, L. M., Simonson, T., and Warren, G. L. (1998) *Acta Crystallogr. D Biol. Crystallogr.* **54,** 905–921
23. Emsley, P., and Cowtan, K. (2004) *Acta Crystallogr. D Biol. Crystallogr.* **60,** 2126–2132
24. DeLano, W. L. (2002) *The PyMOL User's Manual,* DeLano Scientific LLC, San Carlos, CA
25. Quiocho, F. A., Spurlino, J. C., and Rodseth, L. E. (1997) *Structure* **5,** 997–1015